

the growth regime investigated and explained well by the dynamical scaling law.

Registry No. PVDF, 24937-79-9; N117, 119314-70-4.

## References and Notes

- (1) Kyu, T.; Yang, J. C. *Macromolecules*, preceding paper in this issue.
- (2) Kyu, T.; Saldahna, J. M. *J. Polym. Sci., Polym. Lett. Ed.* **1988**, *26*, 33.
- (3) Olabisi, O.; Robeson, L. M.; Shaw, M. T. *Polymer-Polymer Miscibility*; Academic: New York, 1979.
- (4) Gunton, J. D.; San Miguel, M.; Sahni, P. S. In *Phase Transitions and Critical Phenomena*, Domb, C., Lebowitz, J. L., Eds.; Academic: New York, 1983; Vol. 8.
- (5) Yang, J. C. M.S. Thesis, University of Akron, 1989.
- (6) Cahn, J. W. *J. Chem. Phys.* **1965**, *42*, 93.
- (7) Cahn, J. W.; Hilliard, J. E. *J. Chem. Phys.* **1958**, *28*, 258.
- (8) Langer, J. S.; Baron, M.; Miller, H. D. *Phys. Rev. A* **1975**, *11*, 1417.
- (9) Binder, K.; Stauffer, D. *Phys. Rev. Lett.* **1975**, *33*, 1006.
- (10) Siggia, E. D. *Phys. Rev. A* **1979**, *20*, 595.
- (11) Kawasaki, K.; Ohta, T. *Progr. Theor. Phys.* **1978**, *59*, 362.
- (12) Binder, K.; Heermann, D. H. In *Scaling Phenomena in Disordered Systems*; Pynn, R., Skjeltorp, T., Eds.; Plenum: New York, 1985; p 207.
- (13) Furukawa, H. *J. Appl. Crystallogr.* **1988**, *21*, 805.
- (14) Furukawa, H. *Phys. Rev. Lett.* **1979**, *43*, 136.
- (15) Furukawa, H. *Phys. A* **1984**, *123*, 497.

## Optical Properties of Solvent-Cast Polymer Films

J. S. Machell, J. Greener,\* and B. A. Contestable

*Manufacturing Research and Engineering, Eastman Kodak Company, Rochester, New York 14650. Received February 10, 1989; Revised Manuscript Received May 26, 1989*

**ABSTRACT:** The optical properties of solvent-cast films were studied for several polymer formulations over a wide range of casting conditions. It is shown that the casting process induces distinct molecular order in the solid film as manifested by finite birefringence in the cross-film (transverse) direction. The optical anisotropy represents a random molecular alignment parallel to the film plane which can be observed only by measurements in oblique incidence. The level of birefringence depends on the general mode and conditions of the casting procedure and on the optical properties of the polymer. Two distinct procedures, free casting and blade casting, were evaluated and found to produce films with widely varied levels of birefringence. Birefringence was also influenced by the solvent type, the casting temperature, the surface energy of the substrate, and the timing of the peel-off step. In the limit of thin ( $\leq 25 \mu\text{m}$ ) films, the transverse birefringence can be loosely correlated with the intrinsic birefringence of the polymer. Indeed, it is shown that by blending miscible polymers having intrinsic birefringences that are opposite in sign, one can produce effectively nonbirefringent films. Two such blends have been tested in this study. All our observations are interpreted in terms of a molecular "freezing-in" process induced by drying stresses.

## I. Introduction

The optical properties of solvent-cast polymer films are of great technological importance in a host of optoelectronic systems and devices, e.g., in optical waveguides, in optical data storage systems, and in various linear and nonlinear optical components. These properties are generally dictated by the intrinsic optical anisotropy of the polymer chain and by the orientation induced during the casting operation. The alignment of polymer molecules and the corresponding optical anisotropy in solvent-cast films has been addressed by several investigators. General aspects of macromolecular organization in the vicinity of inorganic surfaces have been reviewed by Rickert et al.,<sup>1</sup> who consider in detail three features that control the behavior of polymer molecules near surfaces: (i) substrate properties, (ii) solution organization, and (iii) interfacial properties of macromolecules. All three features contribute, to some extent, to the level of molecular order near solid surfaces, and they underlie the complex nature of the corresponding phenomena.

Cherkasov et al.<sup>2</sup> studied orientation phenomena in polymer films produced by free casting (see next section for definition) and observed that the polymer molecules tend to align parallel to the solid surface in a manner resembling liquid-crystalline (cholesteric) order. They found, however, that the planar orientation has a finite range that depends on the stiffness of the polymer chain. For

stiff backbone polymers the planar orientation zone may extend  $20 \mu\text{m}$  into the film whereas for flexible chain polymers the high orientation zone is only ca.  $1 \mu\text{m}$  thick. Some molecular order, according to Cherkasov et al., may extend well beyond this high orientation "skin" reaching  $10\text{--}50 \mu\text{m}$ . Although the origin of this effect was not fully elucidated, it was speculated that the high orientation arises from steric/adhesion effects and long-range interactions of the solid surface with the polymer molecules.

Prest and Luca,<sup>3,4</sup> in a study on the properties of polymeric films cast from solution by thin, wire-wound, draw bars, also observed high planar orientation in the solid films. They view the molecular ordering process as a competition between planar conformation induced by drying ("drying stress") and the tendency of the molecules to drift toward a random ("equilibrium") conformation. As solvent evaporation proceeds, the molecular mobility in the collapsed film becomes increasingly restricted until the drying-induced conformations are "frozen" in the solid matrix as the glass transition is approached. Prest and Luca studied relatively thin films ( $1\text{--}5 \mu\text{m}$ ) and evaluated the effects of solvent, polymer structure, molecular weight, and drying conditions on the birefringence level in the film. The contribution of drying stresses to the molecular organization in solvent-cast films was also noted by Sudduth and Rogers<sup>5</sup> and Sosnowski and Weber.<sup>6</sup> Cohen and Reich<sup>7</sup> studied the effects of molecular weight

and polydispersity on molecular ordering in thin (1–10  $\mu\text{m}$ ) polystyrene films produced by dip coating. Like Cherkasov et al.,<sup>1</sup> they observed long-range ordering in the films which was attributed to “cooperative phenomena occurring during solvent evaporation as a result of molecular entanglements and unrelaxed conformations...” The effect of increasing molecular weight was to increase the birefringence in the film, in line with the findings of Prest and Luca.

In the present work the previous studies were extended to thicker films (12–200  $\mu\text{m}$ ), other polymer formulations, and different casting techniques. In addition, in order to establish the leading procedural and material factors that control the level of birefringence in the cast film, the effects of the solid substrate, the casting temperature, the solvent type, and the polymer composition (in a miscible blend) were also investigated.

## II. Experimental Section

**A. Casting Procedures.** Polymer films were produced by two distinct methods. The first, free casting (FC), involves casting a polymer solution onto a flat-bottomed glass cup without imposing hydrodynamic stress on the liquid. The solvent is allowed to evaporate under ambient conditions (ca. 22 °C and 60% RH) until the film hardens. The hardened film is then removed from the cup by washing it off with distilled water and placed in a vacuum oven at 100 °C for 12 h for final drying. DSC and gas chromatography data indicated that this procedure was effective in removing residual solvent and moisture from the film. The thickness of films produced by this method is dependent in a straightforward way on concentration and the volume of liquid in the cup. In this study, the concentration was varied in the range 1–8 (wt/wt) % and the liquid volumes ranged from 5 to 20 mL yielding film thicknesses of 12–200  $\mu\text{m}$ . The lower limit is due to difficulties in producing self-supporting films with uniform thickness while attempts to produce films thicker than 200  $\mu\text{m}$  usually led to various gross defects, such as “orange peel”, on the film surface.

In the second method, blade casting (BC), a knife blade was used to spread the liquid over a flat glass substrate. In this process considerable hydrodynamic stresses were generated during the coating step. Since the liquid films produced were relatively thin, initial solvent removal from the cast layer was relatively fast under ambient conditions—the films were hard to the touch within minutes. The coatings were left at ambient for ca. 12 h, and final solvent removal was done by placing the coated substrates in a vacuum oven for 5 h at  $T \approx T_g - 25$  °C. After removal from the oven the coatings were soaked in distilled water, peeled off the substrate, and dried again in vacuo for 2 h at 60 °C. Again, gas chromatography and DSC data indicate that only trace amounts of solvent remained in the films after this intensive drying. It is important to note that the order of peeling the film from the substrate, i.e., before or after drying in the oven, had a significant effect on the properties of the film. The final film thickness was dictated by the blade height and the concentration. The effect of blade height on the thickness of the deposited film can be estimated from the coating dynamics of a slot coater,<sup>8</sup> and the effect of concentration derives from a simple mass balance. The blade height was varied in the range 120–760  $\mu\text{m}$  and the concentrations used were 5–20 (wt/wt) %, producing thicknesses in the range 12–114  $\mu\text{m}$ . Here too the limits were dictated by difficulties in controlling thickness uniformity (for the thin films) and various surface defects (for the thick films). In both methods, but especially in the BC process, air currents above the drying layers and exceedingly fast drying produced “orange peel” defects on the dried films. To circumvent this problem, the BC films were enclosed in a glass box and a lid was placed on the FC cups while the films were drying at ambient. This slowed down the evaporation rate yielding films with good clarity. Some of the films became opaque due to spontaneous crystallization during the initial drying step. This was prevalent in the thick polycarbonate films. When the enclosing box was gradually removed,

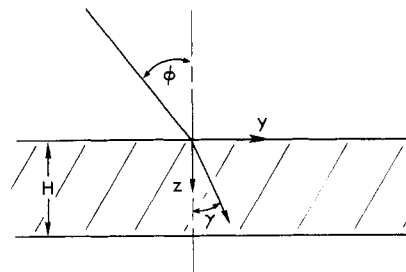


**Figure 1.** A schematic diagram of the film and the incident beam.

the drying rate was increased and the crystallization process could be effectively suppressed.

**B. Birefringence Measurements.** (1) **Procedure.** Birefringence is defined as the difference in refractive index between two orthogonal planes of polarization, and it expresses the level of optical anisotropy of the medium. Generally, three components of birefringence can be defined for any matrix in a Cartesian frame— $-\Delta n_{xy}$ ,  $\Delta n_{xx}$ , and  $\Delta n_{yy}$ , where  $\Delta n_{ij} = n_i - n_j$ . When all the components are zero, the matrix is said to be optically isotropic. The films produced by either of the casting methods were isotropic in the plane of the films; i.e., no preferred orientation was detected in the  $x$ - $y$  plane (see Figure 1), yielding  $\Delta n_{xy} = 0$ . However, the other components of birefringence,  $\Delta n_{xx}$  and  $\Delta n_{yy}$ , were typically nonzero, indicating that some level of molecular order exists in the transverse (in-plane) direction. For this case the two “transverse” components,  $\Delta n_{yy}$  and  $\Delta n_{xx}$ , are equal since  $\Delta n_{xy} = 0$ . Since the cast films are relatively thin, these components cannot be measured directly. General procedures for measuring birefringence in thin films were developed independently by Spence<sup>9</sup> and Stein.<sup>10</sup> The basic technique involves the measurement of birefringence in oblique incidence, i.e., at some angle  $\phi$  relative to the normal to the film plane. If the film is rotated about the  $x$  axis, the two “transverse” components of birefringence are

$$\Delta n_{xy} = \frac{\Delta n_{xy} - \frac{R_\gamma}{H} \cos \gamma}{\sin^2 \gamma} \quad (1)$$

$$\Delta n_{xx} = \frac{\Delta n_{xy} \cos^2 \gamma - \frac{R_\gamma}{H} \cos \gamma}{\sin^2 \gamma} \quad (2)$$

where  $\gamma$ , the refracted angle, is given by (see Figure 1)

$$\gamma = \sin^{-1} ((\sin \phi)/n) \quad (3)$$

with  $n$  being the average index of refraction and  $H$  is the film thickness.  $R_\gamma$  is the apparent optical retardation observed for the oblique angle  $\phi$  and the corresponding refracted angle  $\gamma$ . Equations 1 and 2 are identical since  $\Delta n_{xy} = 0$ . Equation 1 can be rearranged to give

$$(R_\gamma/H) \cos \gamma = \Delta n_{xx}(1 - \cos^2 \gamma) \quad (4)$$

which is the working equation used to obtain  $\Delta n_{xx}$ ; a plot of  $(R_\gamma/H) \cos \gamma$  vs  $\cos^2 \gamma$  yields  $-\Delta n_{xx}$  as the slope. Experimentally, the retardation  $R_\gamma$  is measured for several oblique angles to ensure complete sampling, and the data are fit by linear regression to determine the “transverse” component of birefringence via eq 4.

(2) **Apparatus.** The optical train for measuring birefringence is depicted in Figure 2. The light source is a 1.8-mW HeNe laser polarized 500:1 and filtered by an additional polarizer positioned parallel to the polarized beam. The PMT detector is connected to a voltmeter with a needle readout scale. The polarizer and analyzer are crossed and positioned at  $-45^\circ$  and  $+45^\circ$ , respectively. A Soleil-Babinet compensator placed between the crossed polars acts as a zero-order waveplate with variable retardation which is adjusted by a micrometer screw. When a transparent sample is placed in the light path with its principal axis  $45^\circ$  to the polarizer and analyzer, the retardation of the compensator is adjusted to compensate for the retardation  $R$  in the sample. The difference in the micrometer readings

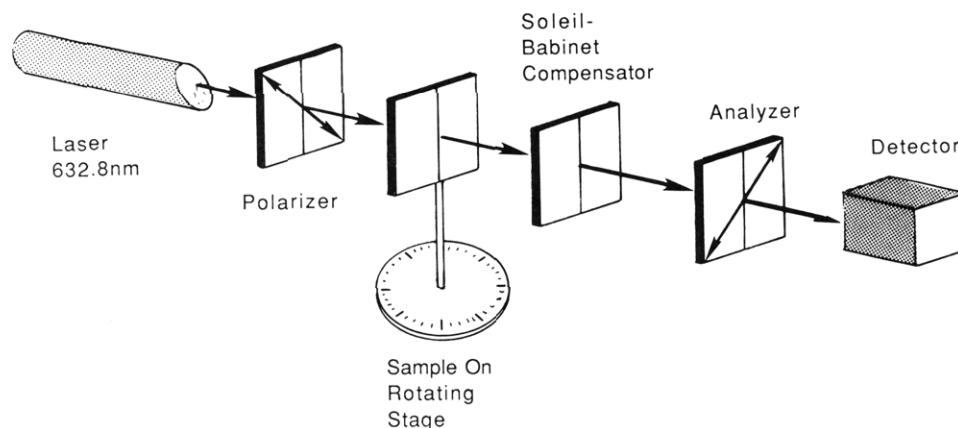


Figure 2. A schematic diagram of the optical setup.

Table I  
Materials

polymer	grade (designatn)	source	$M_w^a$	PD <sup>b</sup>	$T_g^c$ , °C	$\Delta n^d$
bisphenol A polycarbonate	Merlon M50F (PCI)	Mobay	65 300	2.3	154	0.21 <sup>d</sup>
polystyrene	Styron 685D (PS)	Dow	312 300	2.5	107	-0.1 <sup>e</sup>
tetramethyl polycarbonate	(TMBPA)	General Electric	64 600	2.6	198	
poly(2,6-dimethyl- <i>p</i> -phenylene oxide	(PPO)	General Electric	49 000	2.9	210	0.2 <sup>e</sup>

<sup>a</sup> PS equivalents. <sup>b</sup> PD = polydispersity. <sup>c</sup> DSC, 10 °C/min (midpoint). <sup>d</sup> Reference 22. <sup>e</sup> Reference 21.

( $\Delta M$ ) can be converted to birefringence by

$$\Delta n = R/t = \Delta M \lambda / Kt \quad (5)$$

where  $\lambda$  is the wavelength,  $K$  is a calibration factor, and  $t$  is the optical path length in the sample.

**C. Materials.** The polymers used in this study are listed in Table I together with some pertinent properties. The solvent in most of the casting experiments was dichloromethane (DCM). DCM is a good solvent for most of the polymers studied and is also relatively volatile (boiling point 40 °C).

### III. Results

As noted in the previous section, all the films produced by either casting method were isotropic when viewed in normal incidence ( $\Delta n_{xy} = 0$ ) but exhibited varying degrees of optical anisotropy in the transverse direction, i.e.,  $\Delta n \equiv n_{\parallel} - n_{\perp} \neq 0$ , where  $n_{\parallel} = n_x = n_y$  and  $n_{\perp} = n_z$ . Furthermore, the data for both casting methods could be conveniently collapsed into curves of  $\Delta n$  vs  $H$  (dried film thickness), independent of the initial concentration and volume (for FC) or blade height (for BC) used in the casting experiments. These results are in line with the observations of Cherkasov et al.<sup>2</sup> and Prest and Luca<sup>3,4</sup> and suggest that the polymer chains are aligned parallel to the film plane, whereas orientation in the  $x$  and  $y$  directions is completely random. This also implies that the hydrodynamic stresses generated in the BC process did not contribute directly to molecular orientation in the film. The degree of molecular alignment in the plane of the film is dependent on a number of factors to be examined below.

$\Delta n(H)$  curves for PCI films produced by both casting methods under the nominal conditions are presented in Figure 3. The data reveal two striking differences between the casting techniques: First, films produced by the BC method are considerably more birefringent than those produced by the FC method, especially at high  $H$ . Secondly, within the range of the data, the birefringence of the BC films is weakly dependent on thickness whereas, in the FC process, the birefringence drops precipitously with thickness at low  $H$  and then levels off. Similar trends are observed for other polymers. Data for PS and TMBPA are shown in Figure 4, again for both casting methods.

Here, too, the BC films are more birefringent than the FC films, but the slope of the  $\Delta n(H)$  curves is generally milder. Also, in the case of PS, the birefringence of the FC films is nearly independent of thickness, in contrast with the data for PCI. (The precipitous drop in birefringence observed for PCI at low  $H$  occurs possibly at thicknesses outside the data range for PS; i.e., the  $\Delta n(H)$  curve for this material is confined to the high  $H$  asymptote!) The slope of the curve for the TMBPA films produced by FC is also somewhat different from that for PCI, thus indicating that the general shape of the curve as well as the absolute level of birefringence are material-specific. It is finally noted that the birefringence of the PS films is negative whereas the PCI and TMBPA films have positive birefringence. These differences in magnitude and sign are consistent with differences in the intrinsic optical anisotropies of the corresponding polymers.<sup>11</sup>

As noted elsewhere,<sup>12-16</sup> differences in intrinsic birefringence can be exploited to produce nonbirefringent films through blending of miscible polymers with opposite optical anisotropies. PS and PPO and PS and TMBPA are two such polymer pairs.<sup>17-19</sup> The miscibility of these blends was confirmed by DSC runs; for all the compositions studied, DSC scans for both polymer pairs show a single glass transition temperature ( $T_g$ ) which lies between the  $T_g$ 's of the pure components.  $\Delta n(H)$  curves for the PS/TMBPA blends are shown in Figure 5 for various polymer compositions. As for pure PS, the curves are nearly independent of film thickness but the effect of composition is pronounced. This effect is depicted in Figure 6 for both casting methods. The birefringence-composition curve for the BC method is nonlinear, especially at low TMBPA concentration, and full compensation (zero birefringence) is observed at ~40 wt % TMBPA. Werumeus Buning and Gijsen,<sup>15</sup> in a rheo-optical study on the same blend system, have obtained optical compensation at a similar composition (38 wt % TMBPA) and also observed nonlinear dependence of the stress-optical coefficient on composition. However, the coefficient ratio for the pure components reported in their study is substantially different from the birefringence ratio obtained in this work. The absolute value of birefrin-

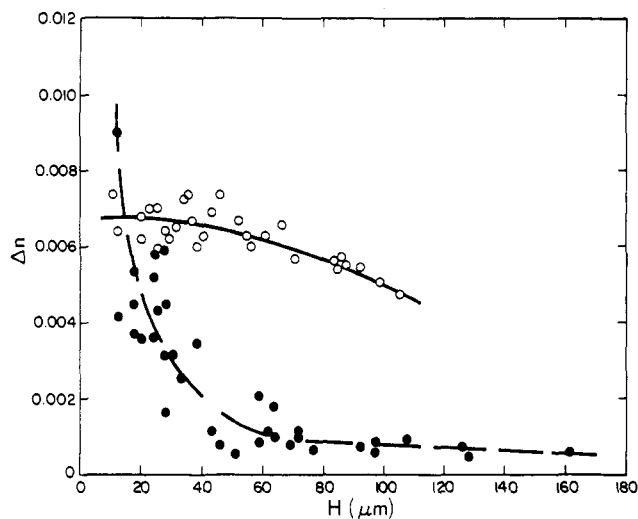


**Figure 3.** Transverse birefringence vs dry film thickness, showing the effect of casting method for PCl cast from DCM: O, BC method; ●, FC method.

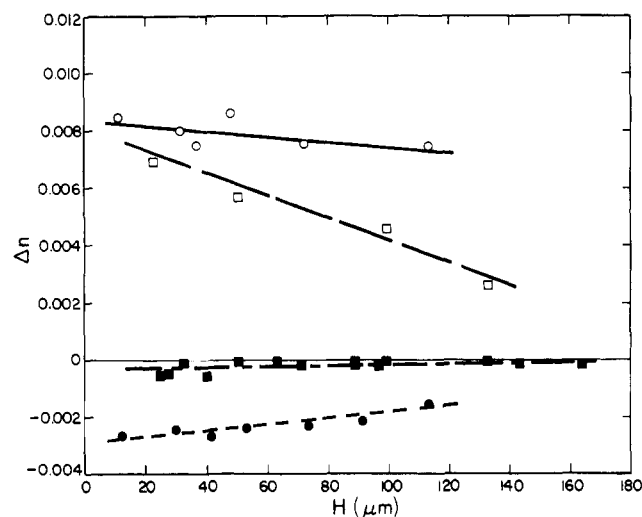


**Figure 4.** Transverse birefringence vs dry film thickness, showing the effect of casting method for PS and TMBPA. TMBPA: O, BC method; □, FC method. PS: ●, BC method; ■, FC method. All films cast from DCM.

gence is systematically lower for the FC method, in line with the data for PCl (Figure 3), but the zero-birefringent composition for this case is not easily discernible because of the low values of birefringence for the PS-rich compositions. The effect of composition for the PS/PPO blend is shown in Figure 7 only for the BC method. This curve as well as the corresponding curve for the PS/TMBPA blend are monotonous but slightly nonlinear. The zero-birefringent composition for the PS/PPO blend (~67 wt % PS) is intermediate between the value reported by Saito and Inoue<sup>14</sup> and the values obtained by Prest<sup>12</sup> and Greener and Machell.<sup>16</sup>

A critical step in the casting procedure was the removal of the film from the substrate. In particular, the order of removal, i.e., before or after oven drying, appeared to have a decisive effect on birefringence, especially in the BC process. Figure 8 illustrates this point by comparing a nominal  $\Delta n(H)$  curve (film removed after drying) with curves corresponding to early removal. The films in the latter category were allowed to dry at ambient temperature for various times and then peeled off the substrate and placed in the oven unsupported for final drying. Generally, films that are removed from the sub-

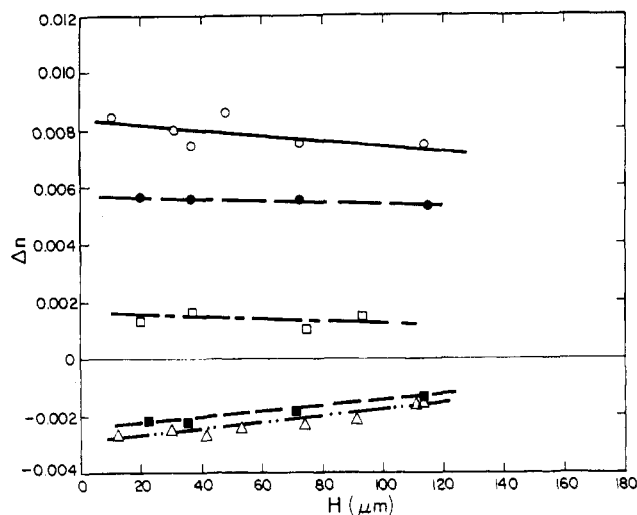


**Figure 5.** Transverse birefringence vs dry film thickness, showing the effect of TMBPA/PS blend composition (wt/wt) (cast from DCM, BC method): O, TMBPA; ●, TMBPA/PS 4/1; □, TMBPA/PS 1/1; ■, TMBPA/PS 1/4; Δ, PS.

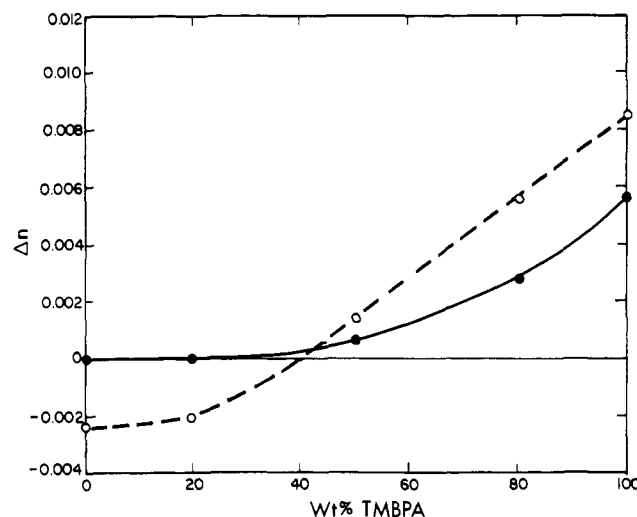


**Figure 6.** Transverse birefringence vs wt% TMBPA, showing the effect of TMBPA/PS blend composition and casting method: O, BC method; ●, FC method. All films cast from DCM.

strate prior to complete drying exhibit significantly lower birefringence, and the effect is more pronounced the shorter the drying time on the substrate. A similar response was exhibited by the PS films. This effect can be correlated with solvent content; although all the films were hard to the touch when removed from the substrate, they contained various amounts of residual solvent. Data obtained by gas chromatography indicate that films dried at ambient contained 2.5–5.0 wt % of DCM, depending on the drying time, whereas films dried in the vacuum oven following the nominal procedure contained <0.1 wt % of DCM. In the case of the FC process the effect of film removal was less pronounced and generally within the scatter of the data (see Figure 9). These results suggest that even small amounts of solvent can cause fast relaxation of stress upon removal of the film from the substrate, leading to a measureable drop in birefringence. Once solvent is completely removed, the polymer molecules are immobilized ("frozen") in their stressed (oriented) conformations. In the FC films the level of stress was inherently low so the removal step per se did not significantly affect the level of birefringence.

The thermodynamic quality of the solvent was studied by Prest and Luca<sup>4</sup> and noted to have a relatively

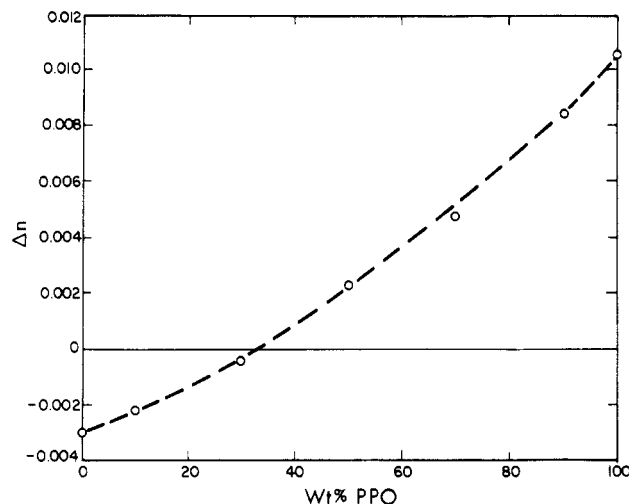


**Figure 7.** Transverse birefringence vs wt% PPO, showing the effect of PPO/PS blend composition. All films cast from chloroform via BC method.

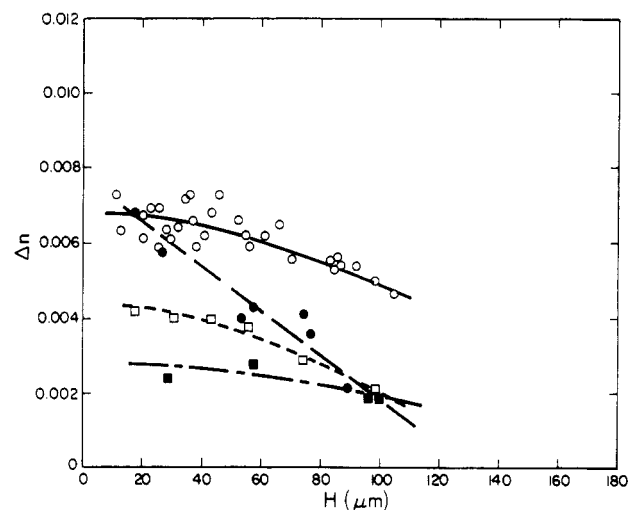


**Figure 8.** Transverse birefringence vs dry film thickness, showing the effect of film removal from casting substrate for PCl (cast from DCM, BC method): O, removed after complete drying at elevated temperature; ●, removed after 24 h at ambient; □, removed after 1.5 h at ambient; ■, removed after 0.5 h at ambient.

small effect on the birefringence level in the cast film. They observed that a slow-evaporating solvent yields lower birefringence due to plasticization of the polymer by the entrapped solvent and a corresponding slower freezing-in process. General confirmation of this observation is provided by the data in Figure 10 where several solvents with a wide range of boiling points (and vapor pressures) are examined. All the solvents are considered generally to be "good" solvents for PC, yet they produce films with varying degrees of orientation. The solvents with the highest boiling points, dioxane (101 °C) and cyclohexanone (155 °C), produced films with systematically lower birefringence. The data for these solvents are limited to relatively thin films due to the onset of crystallization for high  $H$ . (Crystallinity was manifested by distinct haze and a characteristic melting peak in a DSC scan.) The large scatter in the data for these solvents is apparently due to greater sensitivity of the drying process to fluctuations in ambient conditions (% RH, room temperature, etc.). It is also noteworthy that in the case of the FC process the films cast from either dioxane or THF were crystalline at any thickness.

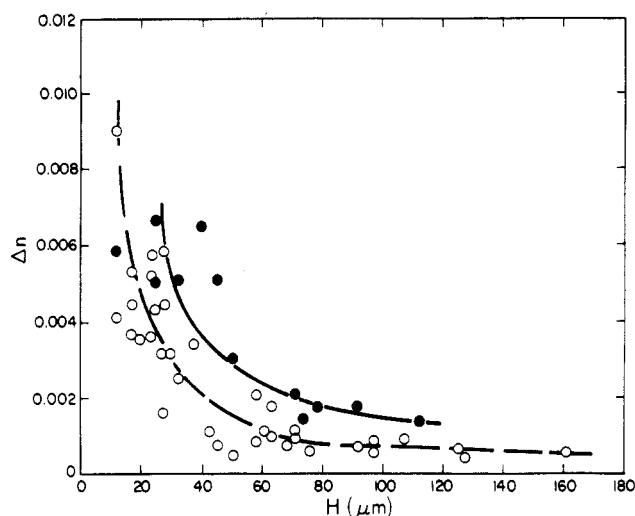


**Figure 9.** Transverse birefringence vs dry film thickness, showing the effect of film removal from casting substrate for PCl (cast from DCM, FC method): ●, removed after complete drying at elevated temperature; O, removed after 1 h at ambient.

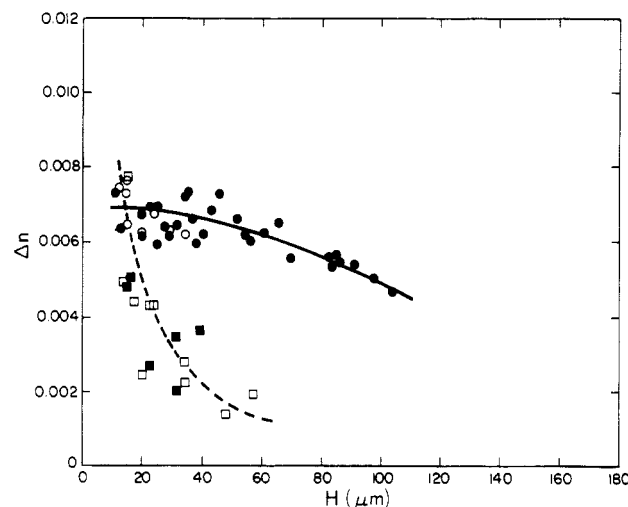


**Figure 10.** Transverse birefringence vs dry film thickness, showing the effect of casting solvent for PCl (BC method): ●, DCM; O, tetrahydrofuran; □, *p*-dioxane; ■, cyclohexanone.

The effect of casting temperature  $T_c$  is shown in Figure 11 for two solvents and two film thicknesses. In all cases the material is PCl and casting was done by the BC process. The casting temperature was varied by pumping water at a specified temperature through an aluminum block under the substrate. The general effect of temperature is to decrease the birefringence although it is considerably less pronounced for dioxane than for DCM. Similar trends were observed by Prest and Luca<sup>4</sup> and attributed to a slower freezing-in process at higher temperatures.

Finally, we consider the role of the casting substrate in controlling the birefringence in the solid film. In all the casting experiments discussed thus far, the substrate for either casting method is a smooth glass surface. In order to evaluate the effect of the substrate, casting experiments were conducted by using Teflon, aluminum, and polyethylene surfaces. The surface energies, as estimated from contact angle data for methylene iodide and water, are 49.4 erg/cm<sup>2</sup> for glass, 49.0 for aluminum, 33.9 for polyethylene, and 20.4 for Teflon.  $\Delta n(H)$  curves for the four substrates are shown in Figures 12–14 for PC, PS, and TMBPA. The data for TMBPA (Figure 14) are for both casting methods while the other sets (Fig-

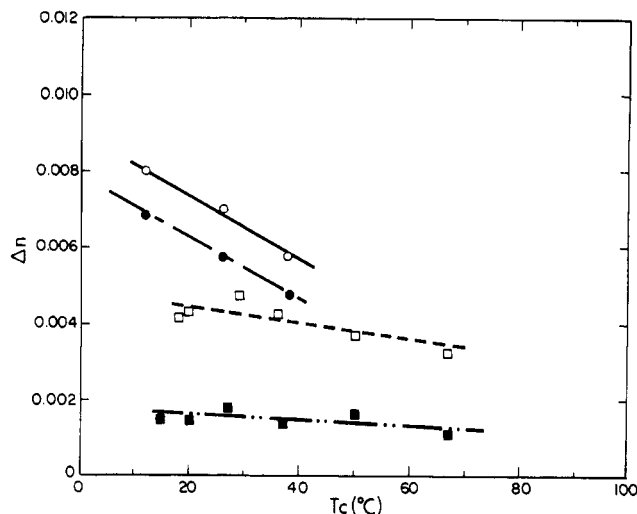


**Figure 11.** Transverse birefringence vs casting temperature, showing the effect of solvent and film thickness for PCI (BC method). DCM: ○, 30 μm; ●, 70 μm. Dioxane: □, 25 μm; ■, 50 μm.

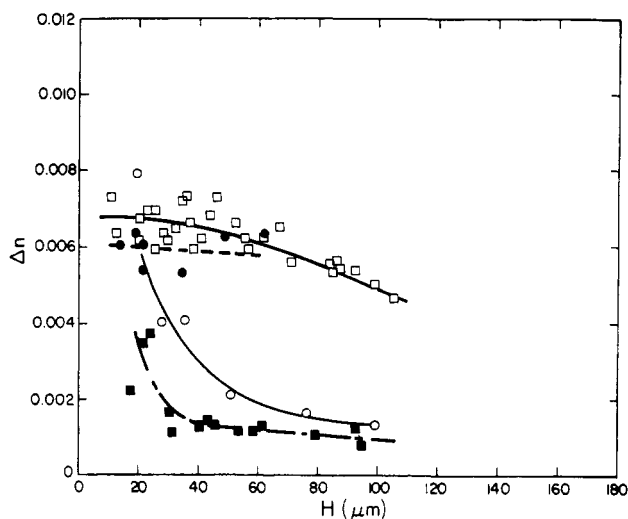


**Figure 12.** Transverse birefringence vs dry film thickness, showing the effect of casting substrate for PCI (cast from DCM, BC method): □, glass substrate; ●, aluminum substrate; ■, Teflon substrate; ○, polyethylene substrate.

ures 12 and 13) are only for BC. A general trend can be clearly discerned from the data: the birefringence of the cast film is substantially reduced with decrease in surface energy of the substrate, and this effect appears to be independent of the casting method or the polymer. It is noteworthy that the effect of a low-energy substrate is qualitatively similar to the effect of early removal of the film from the substrate (Figure 8). Overall, the casting substrate, together with the peel-off step, appears to play a major role in controlling the level of molecular order in the cast film.

#### IV. Discussion

We have already noted that the rapid and inhomogeneous drying during the casting process induces a frozen-in (residual) stress in the solid film that is intimately related to the drying conditions. This stress, in turn, leads to planar molecular order, as manifested macroscopically by the transverse birefringence. The birefringence is simply related to the residual stress via the stress-optical law

$$\Delta n = C \Delta \sigma \quad (6)$$

where  $\Delta \sigma$ , the principal stress difference, is equal to the

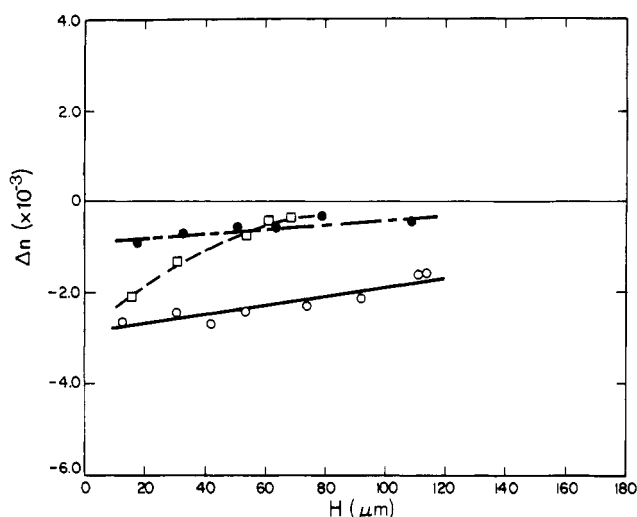


**Figure 13.** Transverse birefringence vs dry film thickness, showing the effect of casting substrate for PS (cast from DCM, BC method): ○, glass substrate; ●, Teflon substrate; □, polyethylene substrate.

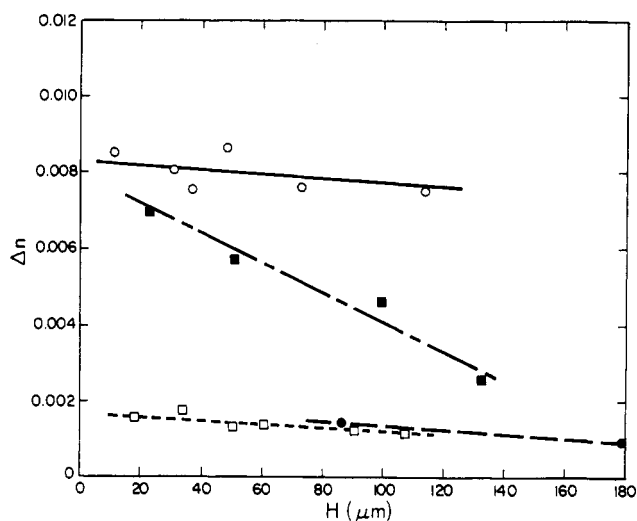


**Figure 14.** Transverse birefringence vs dry film thickness, showing the effect of casting substrate and casting method for TMBPA (cast from DCM). BC method: ○, glass substrate; □, Teflon substrate. FC method: ■, glass substrate; ●, Teflon substrate.

residual plane stress and  $C$  is the operative stress-optical coefficient.  $C$  is generally temperature-independent, but it assumes different values for the polymer glass, its melt, and solution. Although the correct value of  $C$  for use in eq 7 is not obvious, it should scale like the intrinsic optical anisotropy (intrinsic birefringence) of the polymer.<sup>20</sup> This property represents the intrinsic polymer contribution to the transverse birefringence in the film (cf. Figures 4–7). For purely amorphous films, the molecular order can be expressed by the Hermans' orientation function  $f$ :

$$f = \frac{3 \langle \cos^2 \theta_s \rangle - 1}{2} = \Delta n / \Delta n^0 \quad (7)$$

where  $\Delta n^0$  is the intrinsic birefringence of the polymer and  $\theta_s$  is the angle between the main-chain axis and the film plane. For PS,<sup>21</sup>  $\Delta n^0 = -0.1$  and the values of  $f$  for the data in Figure 4 (in the limit of small  $H$ ) are  $\sim 0.03$  and  $\sim 0.003$  for the BC and FC methods, respectively. The corresponding values for PCI<sup>22</sup> and PPO<sup>21</sup> for films produced by the BC method are 0.032 and 0.052, respectively. These values represent generally low levels of molec-

ular order, being much lower for films produced by the FC method than those produced by the BC method. The apparent variability in  $f$  among the various polymers appears to correlate with the temperature interval  $\Delta T_g$  ( $\equiv T_g - T_c$ ) and other factors to be discussed in detail below. It should be noted though that the orientation is expected to vary with position across the film<sup>2</sup> and that the measured values of  $f$  represent spatial averages. In fact, on the basis of previous studies,<sup>2,7</sup> the orientation is expected to be maximum near the substrate-film interface, forming, in effect, a high orientation "skin", and decay toward the free surface. The exact spatial distribution of birefringence could not be inferred directly from our data.

The buildup of stress in solvent-cast films was studied in some detail by Chow et al.<sup>23</sup> and by Croll.<sup>24</sup> In general, drying stresses arise from the volume inhomogeneity induced by the concentration gradient across the film during the drying process. This stress cannot be sustained by the liquid due to its low modulus, but once the polymer vitrifies, the volume inhomogeneity leads to a "frozen-in" stress in the solid matrix. On the basis of ad hoc arguments and in obvious analogy to the thermal stress problem<sup>25</sup> Croll<sup>24</sup> has shown that the average residual plane stress in the film can be expressed by

$$\sigma_R \approx \frac{E}{1-\nu} \frac{\phi_1 - \phi_g}{3} \quad (8)$$

where  $E$  is Young's modulus of the polymer glass,  $\nu$  is its Poisson's ratio, and the term  $\phi_1 - \phi_g$  represents the change in volume upon vitrification.  $\phi_1$  and  $\phi_g$  are respectively the volume fractions of solvent just prior to vitrification and in the glassy ("dry") state.

Equation 8 expresses only the gapwise-averaged stress; the spatial dependence of the residual stress across the film is expected to be complex owing to the complex nature of the drying process.<sup>26-29</sup> Generally, thick liquid films should give rise to large density gradients and thereby induce large instantaneous stresses as in the analogous cooling problem. However, in contrast to the cooling problem, solvent becomes entrapped in the film as solid skin builds up at the free surface and its diffusion out of the film is gradually slowed down. Our data indicate that large amounts of solvent remain in the film a long time (days) after casting is complete if the drying is not sufficiently intensive, i.e., using high temperature and vacuum. This gradual decrease in drying rate will plasticize the polymer and relax some of the stresses already present in the film. This latter effect is expected to dominate the stress buildup process in relatively thick liquid films, and it implies that the gapwise-averaged value of the term  $\phi_1 - \phi_g$  in eq 8 should be lower for thick films. This general argument can be used to explain the difference between films produced by the FC and BC methods. For the same final film thickness,  $H$ , the initial liquid layer thickness,  $H_0$ , in the FC process (500–4000  $\mu\text{m}$ ) is generally much greater than in the BC method (50–400  $\mu\text{m}$ ), and hence, lower residual stress and birefringence are expected for films produced by the former method as is indeed observed experimentally. Only at low  $H$  the results for both methods converge since the corresponding  $H_0$ 's for the FC process approach those of the BC process. Since  $H$  is a linear function of  $H_0$ , the birefringence is expected to vary with  $H$  as well, as shown in Figures 3 and 4 for PCl and PS. If these figures are combined and replotted in terms of the coated film thickness  $H_0$ <sup>30</sup> (Figure 15), the data are shifted and seem to form a single sigmoidal curve for each polymer whereby

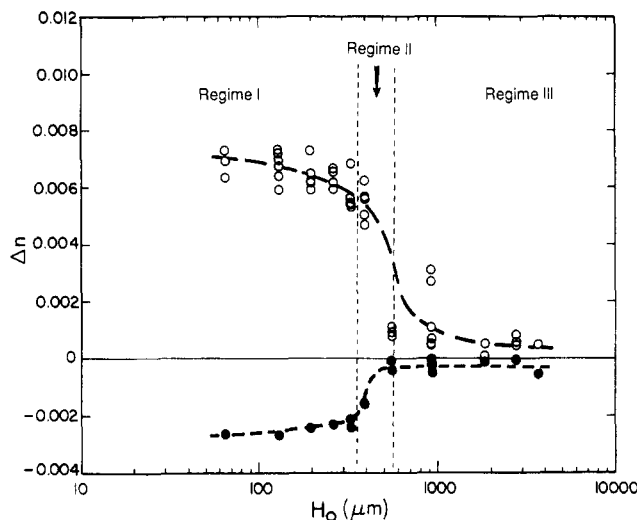


Figure 15. Transverse birefringence vs initial film thickness for films cast from DCM by both methods: O, PCl; ●, PS.

the transverse birefringence appears to have a high asymptote at low  $H_0$  (mostly the BC data) and a low asymptote at high  $H_0$  (the FC data). The level of birefringence in the intermediate range (mostly the FC data) seems to depend on concentration, being higher for less concentrated solutions. It is interesting to note that the inflection point in the  $\Delta n(H_0)$  curve occurs at about the same range of  $H_0$  for both polymers when the same solvent (DCM) is used. The data in Figure 15 suggest that the casting process involves three distinct regimes. At low  $H_0$  (regime I) the birefringence (or stress) is a weak function of  $H_0$  and is effectively controlled by the intrinsic birefringence of the polymer chain. At intermediate  $H_0$ 's (regime II) the birefringence (and residual stress) depends strongly on  $H_0$  as well as on concentration and solvent type. At high  $H_0$  (regime III) the birefringence is relatively low and independent of  $H_0$  and other casting parameters.

The effect of casting temperature can also be explained in terms of the freezing-in mechanism. Although the overall drying rate is increased at higher temperatures, the extent of volume change on vitrification is decreased, and it appears to dominate the molecular ordering process leading to an overall reduction in birefringence (Figure 11);  $\phi_1$ , the dominant term in eq 9, is expected to depend nearly linearly on  $\Delta T_g \equiv T_g - T_c$ .<sup>24,31</sup> The data in Figure 11 together with data for PCl and for the PS/PPO<sup>23</sup> blends can be correlated in terms of the orientation function,<sup>32</sup>  $f$ , vs the temperature interval  $\Delta T_g$ . The correlation, shown in Figure 16 for data in regime I (cf. Figure 15), suggests that  $\Delta T_g$  has a distinct effect on the level of orientation in the film, independent of the polymer system but with a notable dependence on solvent type. The dependence of  $\Delta n$  (or  $f$ ) on  $\Delta T_g$  was first demonstrated for a series of plasticized polystyrenes by Prest and Luca<sup>4</sup> who attribute this behavior to the fact that the rate of the freezing-in process increases monotonically with  $\Delta T_g$ .

Similar arguments can be advanced to explain the solvent effect. The less volatile solvents are slower to leave the film and are therefore more likely to plasticize the polymer and reduce the frozen-in stress as is clearly illustrated by the data in Figure 10. In terms of the mechanism discussed above, the effect of the solvent is 2-fold: first, it may shift the inflection point in Figure 15 (regime II) to lower  $H_0$  with drop in volatility, and, secondly, it may influence the value of  $\phi_1 - \phi_g$  in eq 8. In any case,



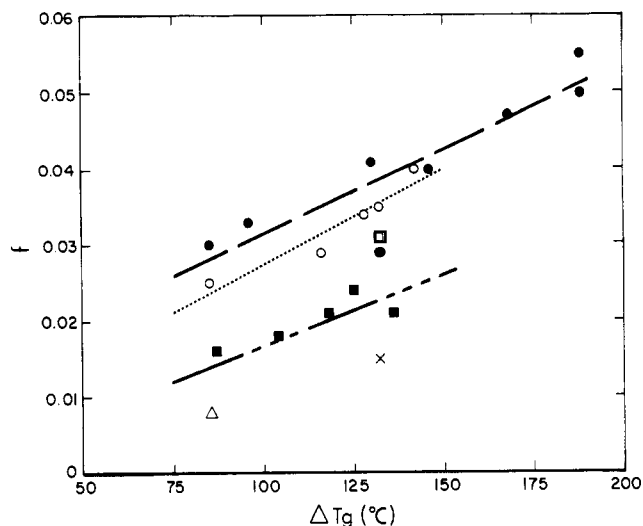


**Figure 16.** Orientation function vs  $\Delta T_g$  for films cast by the BC method at low  $H$  ( $\leq 50 \mu\text{m}$ ). Data are for various polymers and solvents:  $\bullet$ , chloroform;  $\circ$ , DCM;  $\square$ , tetrahydrofuran;  $\blacksquare$ , *p*-dioxane;  $\Delta$ , toluene;  $\times$ , cyclohexanone.

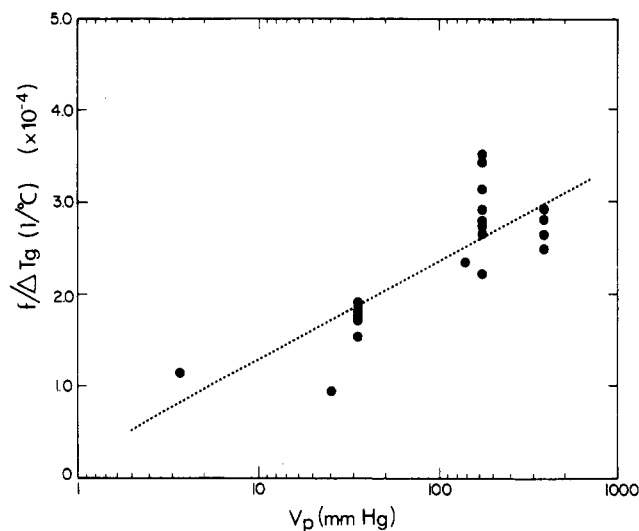


**Figure 17.** Data from Figure 16 replotted as  $f/\Delta T_g$  vs  $\ln V_p$ .

a drop in solvent volatility consistently reduces the level of birefringence in the cast film. The data in Figure 16 can be conveniently collapsed into a single "master" curve by plotting  $f/\Delta T_g$  vs the vapor pressure of the solvent,  $V_p$ , as shown in Figure 17. If the abscissa is logarithmic we obtain, within the scatter of the data, a nearly linear dependence which can be further condensed to

$$f/(\Delta T_g \ln V_p) \simeq (1.2 \pm 0.3) \times 10^{-4} \text{ } ^\circ\text{C}^{-1} \quad (V_p \text{ in mmHg}) \quad (9)$$

where the error,  $\pm 0.3 \times 10^{-4} \text{ } ^\circ\text{C}^{-1}$ , is the standard deviation for the data in Figure 17. This correlation can be used to estimate the intrinsic birefringence of a polymer from measured transverse birefringence for a given solvent ( $V_p$ ) and  $\Delta T_g$ .

The contribution of the substrate to the residual birefringence is inferred from two sets of data. We have shown that the general procedure for removing the film from the substrate and the surface energy of the substrate have a pronounced effect on the transverse birefringence. Chow et al.<sup>23</sup> have speculated that, for the case of a film drying on a rigid support, the interfacial strain dominates the state of stress in the film. In fact, from inspection of the drying problem we expect the residual stress to

vary from zero at the free surface to a maximum at the substrate-film interface. If the interfacial strain is relieved before the polymer is fully vitrified, the stress will be relaxed, leading to lower birefringence. The interfacial strain can be relieved, for example, by "peeling" the film off the substrate while some entrapped solvent is present near the interface (cf. Figure 8). As noted earlier, large amounts of residual solvent were detected in the film a long time after casting if the film was not dried intensively, i.e., in vacuo and at high temperature. Likewise, the surface energy of the substrate is low, as in the case of Teflon or polyethylene (Figures 12–14), and the film will delaminate spontaneously from the substrate due to poor adhesion before solvent is fully removed.

## V. Summary and Conclusions

We have shown that polymer films cast from solution onto a rigid support possess finite birefringence only in the cross-film (transverse) direction which suggests random molecular alignment parallel to the film plane. The corresponding level of birefringence depends on the optical characteristics of the polymer and on the general mode and conditions of the casting procedure. We explored two particular casting methods, free casting (FC) and blade casting (BC), and observed distinct differences in the level of birefringence in films produced by these methods. These differences were attributed to the large variations in the initial thickness of the liquid layer deposited on the casting substrate, which was generally much higher in the FC process, corresponding to three distinct casting regimes (Figure 15). Other factors influencing the birefringence are the solvent type, the casting temperature, the surface energy of the substrate, and the extent of drying when the film is peeled off the substrate. The latter two, having a particularly strong effect on the transverse birefringence, can be readily exploited to manipulate the optical properties of polymer films in a casting operation.

The magnitude (and sign) of birefringence in a cast film is also intimately related to the intrinsic birefringence of the polymer. Indeed, under some conditions, one can use the casting technique to characterize the optical anisotropy of the polymer chain and provide a semi-quantitative assessment of its intrinsic birefringence (see eq 9).

The drying stress mechanism proposed to describe the buildup of molecular order during the casting process explains most of our observations in a consistent manner, and provides a general framework for assessing the effect of various casting parameters on the optical properties of solvent-cast polymer films.

**Acknowledgment.** We thank Dr. D. J. Massa for useful comments and discussions.

**Registry No.** PS, 9003-53-6; PPO (SRU), 24938-67-8; PPO (homopolymer), 25134-01-4; DCM, 75-09-2; (TMBPA)(carbonic acid) (SRU), 38797-88-5; (TMBPA)(carbonic acid) (copolymer), 52684-16-9; chloroform, 67-66-3; tetrahydrofuran, 109-99-9; *p*-dioxane, 123-91-1; cyclohexanone, 108-94-1; (bisphenol A)(carbonic acid) (SRU), 24936-68-3; (bisphenol A)(carbonic acid) (copolymer), 25037-45-0.

## References and Notes

- (1) Rickert, S. E.; Balik, C. M.; Hopfinger, A. J. *Adv. Colloid Interface Sci.* **1979**, *11*, 149.
- (2) Cherkasov, A. N.; Vitovskaya, M. G.; Bushin, S. V. *Visokomol. Soedin., Ser. A* **1976**, *18*, 1628.
- (3) Prest, W. M., Jr.; Luca, D. J. *J. Appl. Phys.* **1979**, *50*, 6067.
- (4) Prest, W. M., Jr.; Luca, D. J. *J. Appl. Phys.* **1980**, *51*, 5170.
- (5) Sudduth, R. D.; Rogers, C. E. *Polym. Lett.* **1973**, *11*, 603.



- (6) Sosnowski, T. P.; Weber, H. P. *Appl. Phys. Lett.* **1972**, *21*, 310.
- (7) Cohen, Y.; Reich, S. *J. Polym. Sci., Polym. Phys. Ed.* **1981**, *19*, 599.
- (8) Greener, J.; Middleman, S. *Polym. Eng. Sci.* **1975**, *15*, 1. See also: Sullivan, T. M.; Middleman, S. *J. Non-Newtonian Fluid Mech.* **1986**, *21*, 13.
- (9) Spence, J. *J. Phys. Chem.* **1939**, *43*, 865.
- (10) Stein, R. S. *J. Polym. Sci.* **1957**, *24*, 383.
- (11) Tsvetkov, V. N.; Andreeva, L. N. *Polymer Handbook*, 2nd ed.; Brandrup, J., Immergut, E. H., Eds.; Wiley: New York, 1975.
- (12) Prest, W. M., Jr. U.S. Pat. No. 4,373,065, 1983.
- (13) Hahn, B. R.; Wendorff, J. H. *Polymer* **1985**, *26*, 1619.
- (14) Saito, H.; Inoue, T. *J. Polym. Sci., Polym. Lett. Ed.* **1987**, *25*, 1629.
- (15) Werumeus Buning, G. H.; Gijsen, R. M. R. *Polym. Prepr. (Am. Chem. Soc.)* **1988**, *29*, 211.
- (16) Greener, J.; Machell, J. S. *J. Appl. Polym. Sci.*, in press.
- (17) Prest, W. M.; Porter, R. S. *J. Polym. Sci., Polym. Phys. Ed.* **1972**, *10*, 1639.
- (18) Wellinchoff, S. T.; Koenig, J. L.; Baer, E. *J. Polym. Sci., Polym. Phys. Ed.* **1977**, *15*, 1913.
- (19) Humme, G.; Rohr, H.; Serini, V. *Angew. Makromol. Chem.* **1977**, *58/59*, 85. See also: Casper, R.; Morbitzer, L. *Angew. Makromol. Chem.* **1977**, *58/59*, 1.
- (20) Treloar, L. R. G. *The Physics of Rubber Elasticity*, 2nd ed.; Oxford University Press: London, 1975; Chapter X.
- (21) Lefebvre, D.; Jasse, B.; Monnerie, L. *Polymer* **1982**, *23*, 706.
- (22) The value of  $\Delta n^\circ$  for PCl (0.21) is taken as the average of values reported in two studies: (a) Biangardi, H. J. *J. Polym. Sci., Polym. Phys. Ed.* **1980**, *18*, 903; *Makromol. Chem.* **1982**, *183*, 1785. (b) Wu, M.-S. *J. Appl. Polym. Sci.* **1986**, *32*, 3263.
- (23) Chow, T. S.; Liu, C. A.; Penwell, R. C. *J. Polym. Sci., Polym. Phys. Ed.* **1976**, *14*, 1311.
- (24) Croll, S. G. *J. Appl. Polym. Sci.* **1979**, *23*, 847.
- (25) E.g.: Struik, L. C. E. *Polym. Eng. Sci.* **1979**, *19*, 223.
- (26) Eaton, R. F.; Willeboondse, F. G. *J. Coat. Technol.* **1980**, *52*, 63.
- (27) Holten-Andersen, J.; Hansen, C. M. *Prog. Org. Coat.* **1983**, *11*, 219.
- (28) Blandin, H. P.; David, J. C.; Vergnaud, J. M.; Illien, J. P.; Malizewicz, M. *Prog. Org. Coat.* **1987**, *15*, 163.
- (29) Croll, S. G. *J. Coat. Technol.* **1987**, *59*, 81.
- (30) The initial film thickness in the BC technique can be estimated as half the blade height (see ref 8).
- (31) Adachi, K.; Fujihara, I.; Ishida, Y. *J. Polym. Sci., Polym. Phys. Ed.* **1975**, *13*, 2155.
- (32) The values of  $\Delta n^\circ$  for the PS/PPO blends were estimated from linear interpolation of the values for the homopolymers (see ref 21).

## Osmotic Pressure of Semidilute Solutions of Flexible, Globular, and Stiff-Chain Polyelectrolytes with Added Salt

Lixiao Wang and Victor A. Bloomfield\*

*Department of Biochemistry, University of Minnesota, St. Paul, Minnesota 55108.  
Received March 24, 1989; Revised Manuscript Received June 7, 1989*

**ABSTRACT:** The renormalization group theory for the concentration dependence of the osmotic pressure of neutral polymers in semidilute solutions is applied to three structural types of polyelectrolytes: flexible chains, exemplified by sodium poly(styrene sulfonate) (NaPSS); compact globular proteins; and stiff chains including DNA, pectinate, and (carboxymethyl)cellulose. Renormalization group theory predicts that the reduced osmotic pressure,  $\Pi M/CRT$ , is a universal function of the reduced concentration  $A_2MC$ , where  $A_2$  is the thermodynamic second virial coefficient and  $M$  is the molecular weight. We have used it to analyze data in the literature on aqueous salt solutions of the three polyion types. The experimental results for NaPSS over a range of salt concentrations from 0.005 to 0.5 M and molecular weight from  $3.2 \times 10^5$  to  $1.2 \times 10^6$  in semidilute solution fall on a universal curve independent of polymer molecular weight, polymer concentration, and salt concentration. The osmotic pressure of the semidilute polyelectrolyte solution in the presence of added salt is very similar to that of neutral polymers in good solvents. The universality of  $\Pi M/CRT$  vs  $A_2MC$  is also observed for globular proteins and stiff-chain macromolecules, with each structural type having its own characteristic curve. The observed high values of the reduced osmotic pressure for spherical proteins at high reduced concentration, compared with the flexible NaPSS, are due to large contributions from third and higher virial terms. Conversely, the low values for the stiff-chain molecules are due to weak contributions from higher virials. Qualitatively, these differences reflect the different interpenetrabilities of these three types of structures.

## Introduction

Polyelectrolyte solutions are complicated. To the variables characterizing neutral polymer solutions—concentration, molecular weight, and solvent quality—must be added ionic strength and polyion charge. Thus, there are additional complications arising from long-ranged polyion–polyion and polyion–small ion electrostatic interactions. Despite these complications, considerable progress can be made in understanding polyelectrolyte solutions. In our previous paper,<sup>1</sup> we showed that renormalization group theory developed for neutral polymers<sup>2,3</sup> could be applied successfully to the diffu-

sional dynamics of polyelectrolytes. In this paper we consider the application of renormalization group theory to the osmotic pressure of solutions of flexible polyelectrolytes. In addition, we consider similar universal relations for globular and rodlike polyelectrolytes, structures of particular interest in biological systems. A similar survey has been undertaken by Burchard<sup>4a</sup> for neutral polymers with these shapes and by Cherayil et al.<sup>4b</sup> for linear, star, and ring polymers.

The osmotic pressure  $\Pi$  of semidilute poly(styrene sulfonate) at various salt concentrations has been measured as a function of polymer concentration  $C$  by Koene et al.<sup>5</sup> They found that at constant salt concentration,